

# The sensitivity of the Seychelles–Chagos thermocline ridge to large-scale wind anomalies

Juliet C. Hermes and Chris J. C. Reason

Hermes, J. C., and Reason, C. J. C. 2009. The sensitivity of the Seychelles–Chagos thermocline ridge to large-scale wind anomalies. – ICES Journal of Marine Science, 66: 000–000.

The Seychelles–Chagos thermocline ridge (SCTR) in the southwest tropical Indian Ocean is important for regional climate, the Madden–Julian Oscillation, as well as upper-ocean nutrients and related phytoplankton and zooplankton densities. Subsurface variability in this region has been proved to influence the overlying sea surface temperatures, which in turn can influence eastern African rainfall. There is evidence that austral summers with a deeper (shallower) SCTR tend to have more (less) tropical cyclone (TC) days in the Southwest Indian Ocean. The importance of this relationship was underlined during the 2006/2007 austral summer, when areas of Madagascar and central Mozambique experienced devastating floods, because of ten named tropical storms, including several intense TCs, effecting on these areas. At the same time, the SCTR during this season was anomalously deep, partly because of a downwelling Rossby wave that propagated across the South Indian Ocean during the previous austral winter/spring. In this paper, a regional ocean model is used to investigate the effect of remote forcing on this region and to study the sensitivity of the SCTR to changes in the large-scale winds over the South Indian Ocean, with a particular focus on the events of the 2006/2007 austral summer.

**Keywords:** Rossby waves, Seychelles–Chagos thermocline ridge, southwest tropical Indian Ocean, upwelling.

Received 15 August 2008; accepted 18 February 2009.

J. C. Hermes: South African Environmental Observation Network, Private Bag X2, Roggebaai 8012, South Africa. Chris J. C. Reason: Department of Oceanography, University of Cape Town, Rondebosch, Cape Town, South Africa. Correspondence to J. C. Hermes: tel: +27 21 402 3547; fax: +27 21 402 3674; e-mail: juliet@saeon.ac.za.

## Introduction

In recent years, substantial progress has been made in understanding the variability of the Indian Ocean. Phenomena such as the Indian Ocean zonal dipole mode (Saji *et al.*, 1999; Webster *et al.*, 1999; Behera *et al.*, 2000) and sea surface temperature (SST) anomalies in the subtropical South Indian Ocean (Behera and Yamagata, 2001; Reason, 2001; Hermes and Reason, 2005) have been demonstrated to have significant influence on the weather and climate patterns of Indian Ocean rim countries. Moreover, Annamalai *et al.* (2005) have demonstrated that local Indian Ocean forcing must be considered along with ENSO in the seasonal forecasting of many regions neighbouring the Indian Ocean.

The Indian Ocean is unique in its oceanography for a number of reasons (see Schott and McCreary, 2001, for a full review), but one of the more pertinent aspects is the lack of equatorial upwelling, because the climatological winds there tend to be westerly rather than easterly. As a result, the warm pool is found in the eastern Indian Ocean (EIO), as opposed to it being in the west in the tropical Atlantic and Pacific. These major differences in the Indian Ocean are driven by the large-scale, land–sea contrasts between the Asian land mass and the Indian Ocean itself, resulting in monsoonal winds and in seasonal reversing of currents north of  $\sim 20^{\circ}\text{S}$ . In an extensive review investigating the dynamics, thermodynamics, and mixed-layer processes in the Indian Ocean, McCreary *et al.* (1993) identified a zonal region of Ekman suction (upwelling) from  $2^{\circ}30'$  to  $14^{\circ}\text{S}$ , which appeared, on the

annual average, to be forced by negative windstress curl resulting in Ekman divergence. This upwelling region is bound in the south by the South Equatorial Current and in the north, during winter, by the equatorial countercurrent and the equatorial jets during the monsoon transition (Rao and Sivakumar, 1998).

However, recent work by Hermes and Reason (2008), who termed this upwelling the “Seychelles–Chagos thermocline ridge (SCTR)”, and Yokoi *et al.* (2008) demonstrated that the upwelling is also apparent during times of positive windstress curl. During these periods, both the beta component of the windstress forcing and remotely forced Rossby waves strongly influence the vertical velocity, and hence the thermocline depth.

The raised thermocline of the SCTR allows for a strong influence of subsurface variability on the SST, thus enhancing its sensitivity to ENSO through westward-propagating Rossby waves (Masumoto and Meyers, 1998; Xie *et al.*, 2002), as well as the Indian Ocean dipole (IOD; Rao *et al.*, 2002). Therefore, there is a high correlation between the variability in the depth of the thermocline and SST (Xie *et al.*, 2002), as well as with sea surface height (Rao and Behera, 2005).

The upwelling of deeper, colder, nutrient-rich water also affects phytoplankton and zooplankton (Gallienne and Smythe-Wright, 2005), with an increase in chlorophyll in the SCTR evident from satellite data. Moreover, fisheries in the SCTR region to the northeast of Madagascar are affected by a raised nutricline and thus by any changes in the upwelling there (New *et al.*, 2005; Vailiard *et al.*, 2009).

The SCTR is a region where the Madden–Julian Oscillation (MJO) is associated with strong SST variability. Vialard *et al.* (2009) established that atmospheric fluxes drive the SST signature of the MJO in this region. They investigated data from an Autonomous Temperature Line Acquisition System (ATLAS) mooring, which suggested that entrainment cooling and horizontal advection did not seem to fluctuate in a systematic way at the time-scales of the MJO, but neither was negligible at their mooring site (8°S 67°E). Duvel *et al.* (2004) suggested that the shallow thermocline in the SCTR region prevents the mixed layer from deepening excessively during wind bursts, enhancing the SST signal associated with the MJO. It has been suggested (Duvel and Vialard, 2007; Vialard *et al.*, 2009) that interannual variability in SCTR thermocline depth can also influence large-scale organized convective perturbations during MJO onset.

The mean SSTs in this upwelling zone are near the critical 28°C, where they can significantly influence atmospheric deep convection. One obvious example concerns tropical cyclones (TCs). On average, approximately nine TCs occur in the southwestern Indian Ocean (SWIO) each year, although there is a large amount of interannual variability (Vitart *et al.*, 2003). Typically, the cyclone season in the SWIO is December–May, and Annamalai *et al.* (2003) established that the influence of thermocline variations on the surface temperature is particularly strong then. The subsurface variability in the SCTR region is correlated with TC days in the region, because when the upwelling is reduced, there is a higher heat content, resulting in the intensification of these storms (Jury *et al.*, 1999; Xie *et al.*, 2002; Reason and Keibel, 2004; Washington and Preston, 2006). The importance of this relationship was emphasized during the 2006/2007 austral summer (and investigated further herein), when areas of Madagascar and central Mozambique experienced devastating floods as a result of a series of intense cyclones and tropical storms. During that cyclone season, there were 99 TC days, compared with 51 in 2005/2006 and 87 in 2007/2008. Oceanic conditions favourable to these storms were related to anomalous conditions in the SCTR and associated Rossby-wave activity.

Given the inherent variability of the Indian Ocean, a better understanding is needed of the sensitivity of the SCTR to changes in both the local and the remote forcing. Although atmospheric factors, such as vertical wind shear and upper level divergence, also strongly influence tropical cyclogenesis, it is likely that years with basin-scale surface wind changes could also lead to anomalous TC behaviour. Similarly, such years are likely to experience significant changes in upper-ocean nutrient content and hence in chlorophyll and fish concentrations.

Birol and Morrow (2001) and Xie *et al.* (2002) drew attention to Rossby-wave propagation in the South Indian Ocean. A better understanding of the sensitivity of Rossby-wave propagation across the South Indian Ocean to regional windforcing and topography is important, because these waves are known to influence the SCTR, the overlying SST and upper-ocean heat content, and hence, TCs in the region (Xie *et al.*, 2002; Hermes and Reason, 2008). Forced by the observed monthly climatological windstresses, Hermes and Reason (2008) used output from a regional ocean modelling system (ROMS) to study the annual cycle of thermocline depth in the basin in relation to that of local and remote forcing. They proved that Rossby-wave propagation makes an important contribution to the SCTR at certain times throughout the year, although its effect can be masked by the regional windstress. Following on from that work, which only used climatological

forcing, the purpose here is to study the response of the SCTR to large-scale anomalies in the surface winds over the South Indian Ocean, as well as the response to changes in remote forcing and topography. The experiments are motivated by the fact that both ENSO (Reason *et al.*, 2000) and the IOD (Saji *et al.*, 1999) result in substantial changes in the surface winds over this basin and that there is evidence that the subtropical anticyclone over this basin has waxed and waned during the past century (Allan *et al.*, 1995). Moreover, climate change projections suggest that this anticyclone may intensify and shift southwards in a warmer climate.

## Model

The free-surface, hydrodynamic ROMS (Shchepetkin and McWilliams, 2005) can represent the annual variability, position, and intensity of the SCTR (Hermes and Reason, 2008). Therefore, it was used here to investigate the sensitivity of this region to large-scale shifts in the South Indian Ocean anticyclone, as well as the influence of remote forcing on the region. As in Hermes and Reason (2008), the ROMS is applied in a tropical Indian Ocean configuration using ROMSTOOLS (Penven *et al.*, 2008). The domain extends from 10°N to 20°S and 40°W to 100°E at  $\frac{1}{3}^\circ$  resolution, with 40 s coordinate vertical levels that are stretched towards the surface. Initial and boundary conditions are from World Ocean Atlas data (Conkright *et al.*, 2002); short-wave radiation, heat flux, and SST monthly climatology are taken from NCEP/NCAR reanalysis (Kalnay *et al.*, 1996). The control run (CON), which was analysed in Hermes and Reason (2008), was forced with monthly mean windstresses computed from QuikSCAT (Liu *et al.*, 1998), whereas the various experiments modified these winds, as illustrated in Table 1.

In RUN-S, the mean winds were shifted south by 2° over the tropical South Indian Ocean (0–15°S), whereas RUN-N consists of the opposite, i.e. a northward shift of the mean winds. Although idealized, these experiments reflect to some extent the large-scale wind anomalies seen during strong *El Niño* (*La Niña*) events, when large anticyclonic (cyclonic) wind anomalies develop over this basin (Reason *et al.*, 2000); and also those on multidecadal scales (Allan *et al.*, 1995). RUN-2 was forced by winds that were doubled in magnitude over the tropical South Indian Ocean relative to the CON to investigate the linearity or otherwise between the wind strength and the SCTR position and strength. Note that these experiments were all based on QuikSCAT winds.

In addition to these experiments, model runs aimed at better understanding the sensitivity of the SCTR to the local topography and the model response to the local and remote windstress forcing were also performed. These experiments were: RUN\_TOPO, the bathymetry of the SWIO was smoothed to a depth of 4500–5000 m, thereby excluding any effects of the Mascarene Plateau and the mid-ocean ridge; RUN\_NCEP, this was forced with NCEP winds, which are of lower resolution than the QuikSCAT winds used in all the other runs; RUN\_2RIDGE, the strength of the winds over the SCTR (15–5°S and 40–65°E) was doubled; RUN\_2EIO, the strength of the winds over the EIO (15–5°S and 80–110°E) was doubled.

At the boundaries of the imposed wind anomalies in each experiment, the wind changes were ramped in time to prevent unrealistic gradients, and smoothing was applied to the modified winds at the equator and at 15°S to remove sharp gradients. These

**Table 1.** Summary of the response of the SCTR to different experimental model runs.

Run name and description	Maximum and minimum thermocline depth	Position of the SCTR	Details
CON: forced with QuikSCAT winds	Maximum: February and October; Minimum: June and December	–	Semi-annual cycle caused by a combination of windstress curl, beta effect, and downwelling Rossby wave
RUN-S: South Indian Ocean high shifted south by 2°	Maximum: March; Minimum: November	Ridge shifted south compared with CON	Ekman pumping follows windstress curl pattern, beta influence weak. Shallower thermocline than CON during August–February, deeper during February–July
RUN-N: South Indian Ocean shifted north by 2°	Maximum: October; Minimum: May	Ridge shifted north	Downwelling during winter because of strong downwelling beta effect and weaker upwelling windstress curl term. Thermocline is deeper than CON throughout the year, particularly during second half
RUN-2: winds doubled in strength	Maximum: February and October; Minimum: May and December	Little change in position, but shallower	Windstress curl strongly conducive to upwelling during March–December, but balanced by downwelling beta effect. Overall, the thermocline remains much shallower than CON, particularly in first half of the year
RUN_NCEP	Maximum: March and September; Minimum: June and December	Weaker semi-annual signal	Deeper thermocline in the austral winter and more confined vertically. Breakdown in Rossby wave not as apparent
RUN_2RIDGE	Maximum: February and October; Minimum: June and December	Little change in position, but shallower	Modulated Rossby waves and local wind allowing for a shallower thermocline
RUN_2EIO	Maximum: February and September; Minimum: May and December	Slightly shallower over ridge and much shallower in EIO, forming a zonal region of upwelling	Dominant semi-annual signal owing to stronger Rossby waves arriving from east

experiments began from the end of the 10-year CON and were integrated for a further 10 years in each case.

Further runs performed over a larger domain, including the eastern boundary of the Indian Ocean, made little difference to the results, because the boundary conditions applied include the signature of this part of the Indian Ocean, as well as that for the Indonesian through-flow. However, to have full confidence in the results, a high-resolution, global-ocean model should be used.

### Sensitivity of the SCTR region to large-scale wind anomalies over the South Indian Ocean

Figure 1 shows regions of reasonably shallow thermocline depth (<90 m) and the magnitude of the windstress curl for summer and winter in each case. Note that the shallow thermocline region tends to be more zonally extensive during the austral winter than in summer in each experiment. In almost all areas of shallow thermocline during the austral winter, the curl is upwelling favourable (negative in the southern hemisphere). Despite this general similarity, noticeable differences in the thermocline depth exist between the runs.

The most obvious difference from CON occurs for RUN-N. The corresponding weakening in the negative curl results in a smaller area of shallow thermocline compared with CON, and the southern (but not northern) boundary in RUN-N is shifted north. RUN-S reveals a rather similar distribution of the shallow thermocline to CON, except that its southern boundary is also shifted south. Doubling of the wind strength (RUN-2) results in a more zonally extensive region of shallow thermocline, and, as expected, the thermocline is relatively shallower everywhere compared with CON. Therefore, in the austral winter, the SCTR responds more or less linearly to large-scale wind anomalies through changes in local Ekman pumping. However, in the austral

summer, there are much larger areas in each experiment where regions of shallow thermocline depth occur over areas of positive curl. It is the planetary beta effect (Hermes and Reason, 2008; Yokoi *et al.*, 2008) that results in upwelling in regions of positive windstress curl. The relative contribution of the two components of Ekman pumping (windstress curl and beta effect) is discussed later.

Another way of assessing the relationship between the winds and thermocline depth is to plot the annual cycle of the meridional gradient of the thermocline depth averaged over 45–75°E between 15°S and the equator (Figure 2). The thick black line marks where the gradient becomes zero, and generally corresponds to the centre of the SCTR. The strength of the ridge in each experiment can be approximated by the change in this meridional gradient. Moving northwards from the southern boundary (15°S) in CON and RUN-2, the gradient is positive, but weakens towards zero as the thermocline gets shallower and the temperature decreases. Moving farther north from the thick black line in the plot, the gradient gradually becomes more negative as the thermocline gets deeper and the temperature becomes warmer. The gradient in RUN-2 is ~2–3 times greater than in CON, but the centre of the ridge holds a similar position for most of the year, except during the austral autumn.

RUN-S results in a non-linear response in that the first half of the year exhibits a weaker positive gradient than CON in the southern part of the domain (Figure 2), whereas, north of the centre of the SCTR, the negative gradient is stronger than in CON during the second half of the year. In both seasons in RUN-S, the core of the SCTR is located south of its position relative to CON. In RUN-N, a more complex response is evident, with the gradient south of the SCTR centre substantially stronger than in CON in autumn and winter. During winter and spring, the

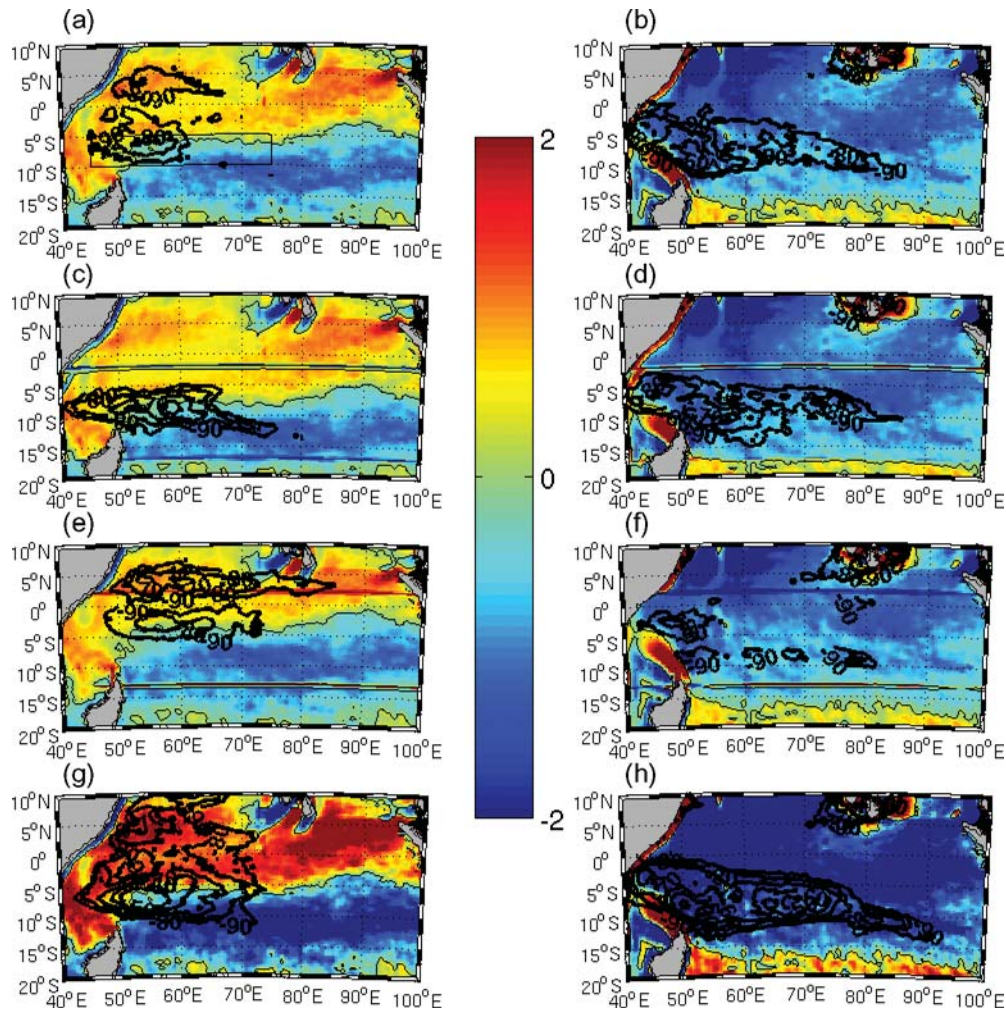


**Figure 1.** (a) QuikSCAT windstress curl ( $\text{N m}^{-3}$ ) with the minimum thermocline depth contours (70, 80, 90 m) for December–January–February of CON. The box highlights the region used for subsequent calculations; (b) as in (a), but for June–July–August; (c) as in (a), but for RUN-S; (d) as in (c), but for June–July–August; (e) as in (a), but for RUN-N; (f) as in (e), but for June–July–August; (g) as in (a), but for RUN-2; (h) as in (g), but for June–July–August.

gradient immediately north of the ridge centre becomes more strongly negative.

The key to the thermocline depth behaviour in both CON and the observations is a strong semi-annual cycle. Figure 2 implies that two maxima/minima in the SCTR depth should exist between 5 and 10°S in CON and RUN-2, but that it is hardly present in RUN-S and RUN-N. Figure 3a, which shows the plots of the monthly mean depth of the 20°C isotherm averaged over the box of 5–10°S × 45–75°E for each run, illustrates that this semi-annual cycle vanishes (strengthens) in RUN-S and RUN-N (RUN-2) and that the annual signal has a much stronger amplitude in RUN-N and RUN-2 than in the other two runs. In addition, like in CON, the months of deepest thermocline during RUN-2 are in February and October. However, in RUN-N, there is only one maximum depth, in October, with the minimum in thermocline depth occurring a month before CON, in May. In RUN-S, the maximum in thermocline depth, in March, appears a month later than in CON. A rapid shoaling then occurs, with an almost constant minimum in thermocline depth from June to December.

These results are important, because they imply that the time of maximum SST over the South Indian Ocean in general (March) might not always coincide with the time of maximum depth (and hence upper-ocean heat content) in the western part of the SCTR or with the months of climatological peak TC activity (January–February) in the Southwest Indian Ocean. Although it is impossible to draw general conclusions about tropical storm activity and thermocline depth variations from Figure 3a (because atmospheric factors, such as vertical wind shear and upper level divergence, also strongly influence cyclogenesis and storm tracks), it is likely that years with these sorts of surface wind variations will have anomalous TC behaviour. Similarly, such years are likely to experience significant changes in upper-ocean nutrient content and hence in chlorophyll and fish concentrations.

To gain insight into the relative contributions of the various forcing terms, the annual cycle of the model vertical velocity, the total Ekman pumping term (i.e.  $\text{curl } \tau + \beta \tau^x / \rho_0 f^2$ ), and the contribution of remote forcing (e.g. caused by Rossby waves) are plotted, as illustrated in Figure 3b–d. Remote forcing is calculated as the difference between the actual model vertical velocity and the

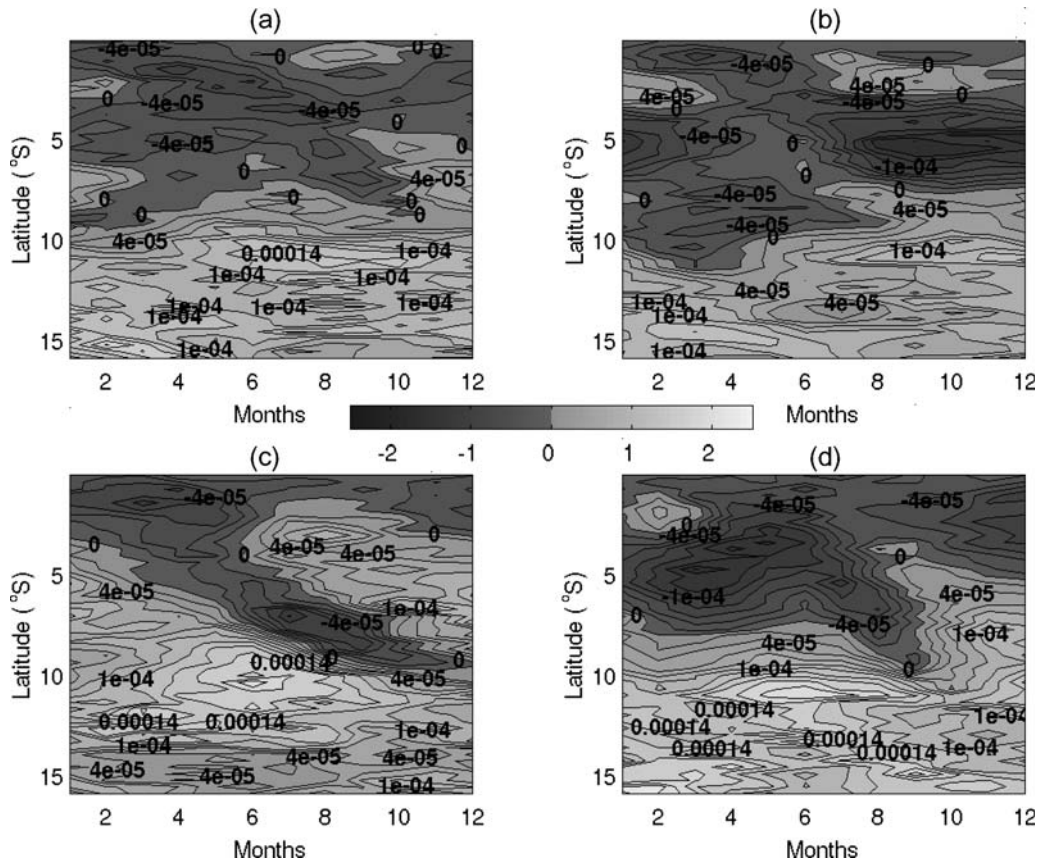


**Figure 2.** (a) Annual cycle of the meridional gradient of the 20°C isotherm depth-averaged over 45–75°E for CON. The thick black line marks the zero gradient; (b) as in (a), but RUN-S; (c) as in (a), but for RUN-N; (d) as in (a), but for RUN-2.

Ekman pumping term. The various terms are calculated as spatial averages over the 5–10°S × 45–75°E box corresponding to the western core of the SCTR. Hermes and Reason (2008) examined the annual cycle of the various terms in CON, whereas here we consider how they are changed in the cases with anomalous wind-forcing. The essential character of the annual cycle of these terms is least changed in RUN-2, although there is roughly a 1-month shift in the time of shallowest thermocline and the magnitudes of the various terms are larger.

RUN-N displays behaviour similar to CON for each term during the winter half of the year, but is rather different during the summer half. This similarity during April–September likely results from the fact that easterlies are dominant over most of the South Indian Ocean to ~30°S during these months; therefore, a 2° northward shift does not change the resulting curl all that much. Conversely, equatorial westerlies begin to develop in October and become evident north of Madagascar in summer. In RUN-N, these westerlies develop later in the year and do not extend to near northern Madagascar in summer; therefore, the resulting windstress curl for the summer half of the year will differ more obviously from CON at that time. As illustrated in Figure 3f, the contribution of the windstress curl forces a negative model vertical velocity in CON from mid-December to mid-February, whereas it remains positive in RUN-N.

The other panels in Figure 3 illustrate the annual cycle of the contributions to the vertical velocity over the 5–10°S × 45–75°E box. Note that the sum of the beta effect (Figure 3e) and the

windstress curl (Figure 3f) represents wind-induced vertical velocity. In RUN-S, the 2° southward shift in mean winds emphasizes the contrast between the low-latitude westerlies and the subtropical easterlies during the summer half of the year. In the winter half of the year, the change in wind direction over the tropical central and western South Indian Ocean from southeasterly to southerly near the equator in CON will now extend 2° farther south. These changes in wind direction mean that RUN-S has rather different Ekman pumping patterns from CON (Figure 3c), so the character of the annual cycle of the SCTR in Figure 3a is more different from CON than is the case for either RUN-N or RUN-2.

All runs reveal a semi-annual variation in the contribution of the local Ekman pumping terms to the vertical velocity (Figure 3c), but these cycles are weaker (stronger) in RUN-S (RUN-2 and to a lesser extent in RUN-N). RUN-N and CON have similar magnitudes in the beta effect (Figure 3e), whereas RUN-S has a much smaller contribution of the beta effect to the Ekman pumping, particularly in winter, when there is less contribution of this term to downwelling than in CON. During the austral summer, there is a reduction in the contribution of the beta effect to upwelling in RUN-S compared with CON. The contribution of the beta effect to the Ekman pumping in RUN-2 is considerably larger than in the other runs, because it depends linearly on the magnitude of the zonal windstress component.

The contribution of the windstress curl to the Ekman pumping (Figure 3f) again exhibits the largest amplitude annual cycle in

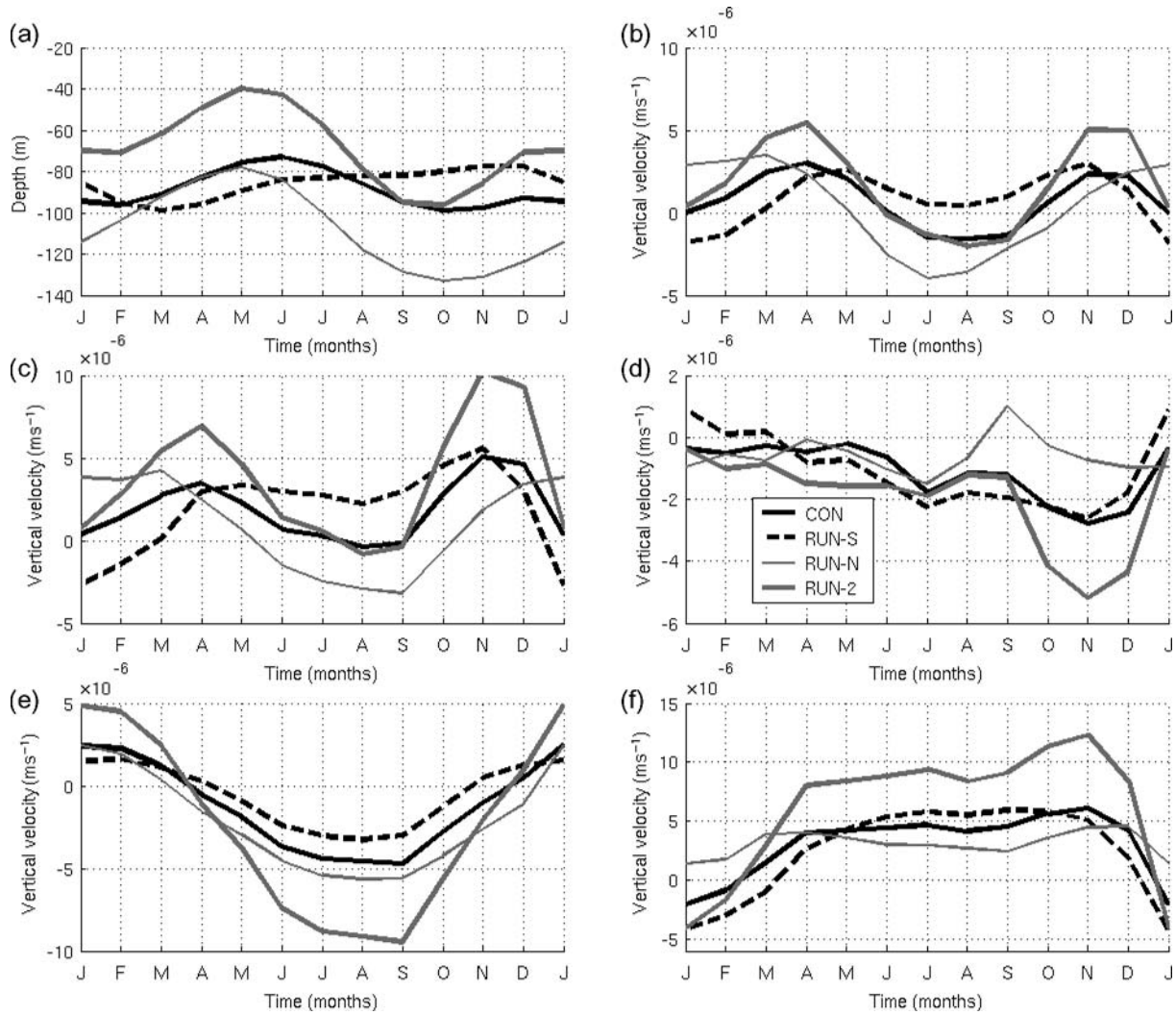


**Figure 3.** (a) The annual cycle of the depth (m) of the 20°C isotherm for each run, averaged over the box illustrated in Figure 1 (45–75°E 5–10°S); (b) as in (a), but the actual model vertical velocity ( $\text{m s}^{-1}$ ), positive values indicate upwelling; (c) as in (a), but the contribution of Ekman pumping (beta+ windstress curl) to the vertical velocity ( $\text{m s}^{-1}$ ); (d) as in (c), but for the contribution of remote forcing to the vertical velocity ( $\text{m s}^{-1}$ ); (e) as in (c), but for the contribution of the beta effect to the vertical velocity ( $\text{m s}^{-1}$ ); (f) as in (c), but for the contribution of the windstress curl to the vertical velocity ( $\text{m s}^{-1}$ ).

RUN-2. This amplitude is weakest in RUN-N, because the northward-shifted winds result in a smaller curl developing between the equatorial westerlies and the trade winds to the south, unlike for CON or RUN-S. In RUN-S, the maximum thermocline depth in March (Figure 3a) arises from a close to maximum downwelling contribution by the windstress curl (in January) combined with a weakening upwelling favourable beta effect. This contribution then results in the maximum thermocline depth during March, because the depth of the thermocline lags the peak in the vertical velocity by  $\sim 2$  months.

In the austral winter, the windstress curl is negative over the box in each case; therefore, its contribution to Ekman pumping is positive and conducive to upwelling (Figure 3f). RUN-S reveals a stronger downwelling influence from the remote forcing term (Figure 3d) than for the other runs. However, the downwelling contribution from the beta effect (Figure 3e) is smaller in RUN-S than in the other cases, so the upwelling Ekman pumping term (Figure 3c), although larger than in the other

runs, is not as big as it otherwise would be. During winter, the Ekman pumping term (Figure 3c) in RUN-N is in fact favourable for downwelling, consistent with the smaller region of shallow thermocline in Figure 1. The Ekman pumping in RUN-2 during OND implies very strong upwelling. However, the effect of this upwelling is reduced because of the presence of a strong downwelling Rossby wave (Figure 3d). To explore the influence of Rossby waves further, the second set of experiments was performed.

### Rossby-wave propagation

The first set of experiments focused on large-scale wind changes over the Indian Ocean and their effect on the SCTR. However, this region has also been strongly affected by remote influences, because of the passage of Rossby waves (Biol and Morrow, 2001; Vinayachandran *et al.*, 2002; Xie *et al.*, 2002), especially during ENSO and IOD events. To investigate the effect of remote forcing on the SCTR, the second set of experiments was performed, as described in the Model section.

The Hovmöller plot for the CON analysed in Hermes and Reason (2008) indicated a “breakdown” in the Rossby-wave propagation across the tropical South Indian Ocean in the 5–10°S band near 60–65°E, which is more obvious when QuikSCAT (Figure 4a and f) winds rather than the coarser NCEP winds were used to force the model (Figure 4c and h). This result suggests that the Rossby-wave propagation may be sensitive to both the local topography (the Mascarene Plateau) and to local and/or regional windstress fields, motivating the need for RUN\_TOPO. Such a breakdown has also been identified in previous work, but for higher latitudes (11–20°S; Wang *et al.*, 2001; Matano *et al.*, 2002).

Wang *et al.* (2001) used altimeter data and idealized model runs to look at the annual cycle at 11°S and 16°S and established that it consists of Rossby waves and the wind-driven localized response. They implied that the two local maxima seen at 11°S and 16°S in the annual cycle are the result of constructive interference between the Rossby waves and the localized response, and that the mid-ocean minimum (near 80°E) is due to destructive interference. The latter is displayed as an abrupt change in the phase of the annual harmonic in this region. At similar latitudes, CON demonstrates a similar breakdown in the westward propagation of the Rossby waves (Hermes and Reason, 2008). However, the

core of the SCTR is farther north, with the peak in upwelling located between 5 and 10°S.

To characterize the temporal structure of the seasonal variability of the SCTR further and to investigate the spatial structure, an annual and semi-annual harmonic was fitted to the model data for CON (Figure 5a–d) over a larger area than that in the study by Wang *et al.* (2001). The annual harmonic and phase compares well with previous modelled and observed results (Masumoto and Meyers, 1998; Rao and Sivakumar, 2000; Wang *et al.*, 2001; Matano *et al.*, 2002), although the amplitude is generally larger in the model, possibly because of the climatological forcing used. A strong maximum in amplitude is present at ~8°S in the eastern tropical Indian Ocean, extending westwards from 100°E to 75°E. Another maximum is seen to the southwest at 50–65°E 10–14°S. These two maxima are separated by an NW/SE orientated region of minimum amplitude. The phase demonstrates a westward movement of the annual cycle that takes two cycles to cross the basin.

The semi-annual harmonic plot (Figure 5b) displays a maximum near and south of the equator between 45 and 65°E, near the position of the mid-ocean minimum in the annual harmonic. Rao and Sivakumar (2000) also found a signal in their second harmonic of temperature at 50 m in this region and

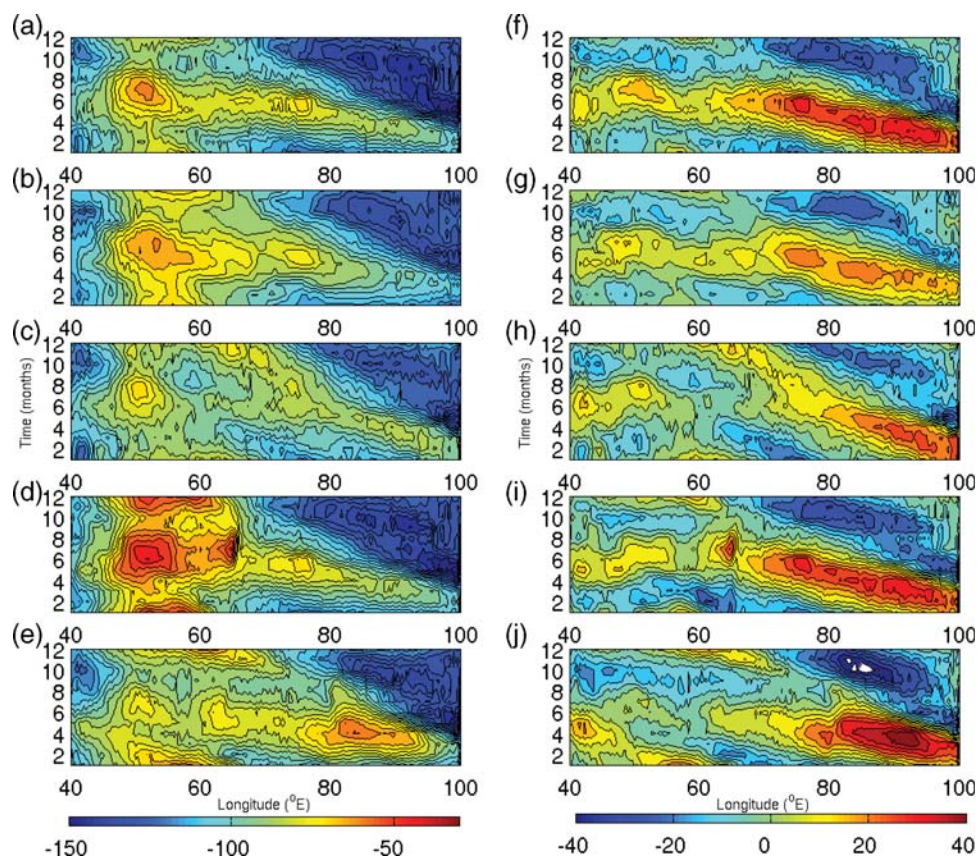


**Figure 4.** (a) Hovmöller plot of the depth (m) of the model RUN\_CON 20°C isotherm over the South Indian Ocean, averaged over 5–10°S. Contour interval is 5 m. Positive values denote a shallower depth and hence upwelling; (b) same as in (a), but for the RUN\_TOPO; (c) same as in (a), but for the RUN\_NCEP; (d) same as in (a), but for the RUN\_2RIDGE; (e) same as in (a), but for the RUN\_2EIO; (f) same as in (a), but Hovmöller plot of the depth (m) of the monthly 20°C isotherm anomaly from the climatology the South Indian Ocean for RUN\_CON; (g) same as in (f), but for the RUN\_TOPO; (h) same as in (f), but for the RUN\_NCEP; (i) same as in (f), but for the RUN\_2RIDGE; (j) same as in (f), but for the RUN\_2EIO.

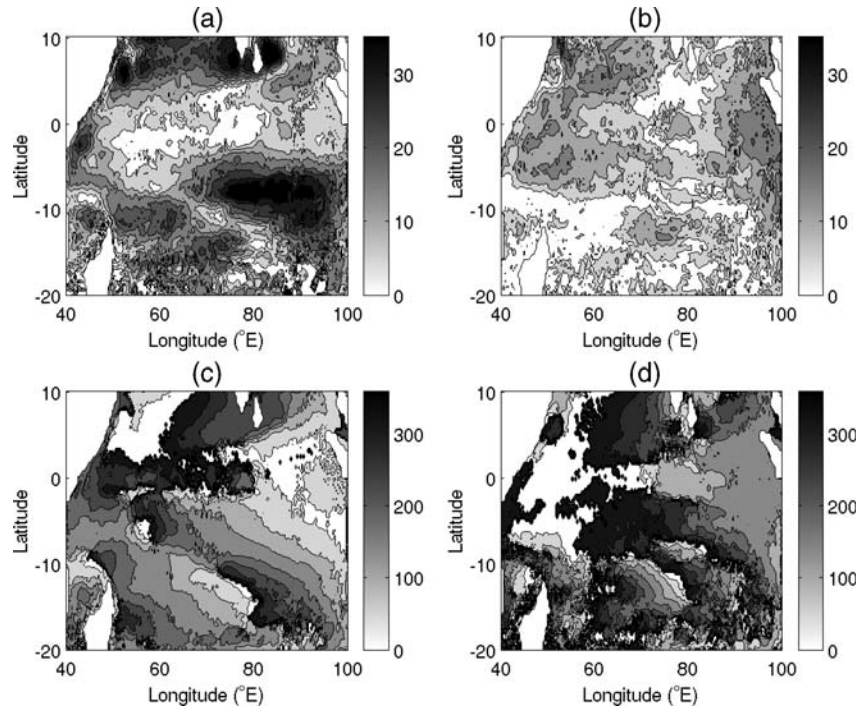


**Figure 5.** (a) The amplitude of the annual harmonic of the CON, the contour interval is 10; (b) same as in (a), but for the semi-annual harmonic; (c) same as in (a), but for the phase of the annual harmonic, the contour interval is 45; (d) same as in (c), but for the semi-annual harmonic.

attributed such a semi-annual signal to the latitudinal movement of the South Indian Ocean subtropical gyre. A semi-annual signal was also established by Sakova *et al.* (2006), along with an 18–24 month signal, one that is also apparent in wavelet analysis of our model data (not presented). Figure 5 reveals how complicated the SCTR actually is, with the southern and eastern regions dominated by the annual cycle, while the northwest part of the ridge is dominated by the semi-annual harmonic.

The region of interest here is slightly farther north than the region on which Wang *et al.* (2001) focused and has been proved to be strongly influenced by both annual and semi-annual cycles, as described above and by Hermes and Reason (2008) and Yokoi *et al.* (2008). The semi-annual harmonic analysis illustrated in Figure 5b and d highlights the dominance of the semi-annual signal in the SCTR. Figure 5c also indicates that the phase change in the annual harmonic occurs farther west at lower latitudes, so in the region of the SCTR, the phase change is closer to 60°E. The phase of the semi-annual harmonic has a similar abrupt phase change to the annual harmonic, but it takes three cycles to cross the basin. These phase changes suggest Rossby-wave propagation.

To investigate the effect of the bottom topography on the westward propagation of these waves, the model was run with smoothed topography. RUN\_TOPO (Figure 4b and g) reveals only a relatively small difference in the nature of the Rossby-wave propagation when compared with the CON (Figure 4a and f). The overall temporal and zonal change in the depth of the thermocline is smoother, and the austral summer upwelling is slightly more enhanced. These rather small differences suggest that changes in the windstress forcing may be more important than the topography. Wang *et al.* (2001) discussed the

effect of interference between localized forcing and Rossby waves at higher latitudes than the SCTR, as opposed to the effect of bottom topography. However, they also suggested that the passage of Rossby waves might also be affected by a special structure of the thermocline. This structure could act as an equivalent bottom topography to scatter the Rossby wave, considering that Rossby waves propagate in the large-scale background thermocline (Wang *et al.*, 2001). Given the defined shoaling of the thermocline in the SCTR, it is quite possible that it could affect the westward propagation of the Rossby waves.

More obvious differences from CON are evident in Figure 4c and h, where the model was forced with NCEP winds, RUN\_NCEP. The core of the SCTR is located slightly farther to the west in this run, and the overall depth of the thermocline is deeper than in CON, most noticeably during the austral winter. In addition, the amplitude of the annual and semi-annual cycle is reduced compared with CON (not presented).

Given that the windstress forcing could be more important than the topography, two other experiments were performed, where the strength of the mean winds was increased over regions thought to be important for the SCTR. RUN\_2RIDGE, where the local winds over the ridge itself (15–5°S and 40–65°E) were doubled in strength, is displayed in Figure 4d and i. In this case, there are large differences in thermocline depth west of 65°E. The upwelling is enhanced throughout the year, and during the austral winter, the core part of the SCTR extends farther to the east. The amplitude of the seasonal signal remains approximately the same as in CON, but the semi-annual cycle is more dominant (not presented). In general, the SCTR depth is reduced in RUN\_2RIDGE, compared with the control case. This shoaling of the SCTR in RUN\_2RIDGE must arise directly from the changes

to the local windforcing over the ridge and its modulation on the Rossby waves from the east arriving in the region, because no other change had been made to the forcing. The stronger winds imposed over the ridge act to reduce the temperatures in the upper ocean, consistent with a shallower SCTR.

In RUN\_2EIO, where the winds are doubled in strength over the EIO (15–5°S 80–110°E), Figure 4e and j indicates that, in the core SCTR region of 50–65°E, the upwelling is stronger than CON during the austral spring/summer and weaker during the austral winter. Because the winds over the ridge were not changed from the CON, this difference in the core SCTR region must arise from remote forcing. Strengthening the winds in the EIO results in a stronger contrast between the easterlies and the northeast monsoon in spring/summer in RUN\_2EIO, compared with the control, so these seasons exhibit the largest differences in upwelling (Figure 4e and j). Farther east, near 80–95°E, there is a strong difference from RUN\_CON in the austral autumn and winter, when the climatological easterlies south of Java begin to strengthen substantially as they feed into the developing Asian monsoon at this time of the year. Doubling the strength of the winds here effectively increases the curl between these

easterlies and the monsoonal westerlies farther north, resulting in increased upwelling in RUN\_2EIO. In the austral spring and summer, the mean curl in this region is weaker so there is a less noticeable effect on the thermocline depth.

### Case study

At the beginning of 2007, a number of severe TCs brought large-scale devastation to Madagascar and parts of Mozambique. It is interesting that just before the cyclone intensification, the surface water in the region of the SCTR was anomalously warm (Figure 6a). This is consistent with the study of Xie *et al.* (2002), who found a connection between the number of cyclone days in the SWIO and the depth of the SCTR. During the 2006/2007 cyclone season, aside from two category 1 cyclones and a number of moderate and severe tropical storms, there were four category 4 cyclones and two category 3 cyclones, and a total of 99 TC days (calculated as the total of the period, in days, of each cyclone) compared with 51 in 2005/2006 and 87 in 2007/2008.

This warming of the SCTR in early 2007 can be linked to the arrival of a downwelling Rossby wave from the southeast tropical Indian Ocean, where easterly wind anomalies persisted from

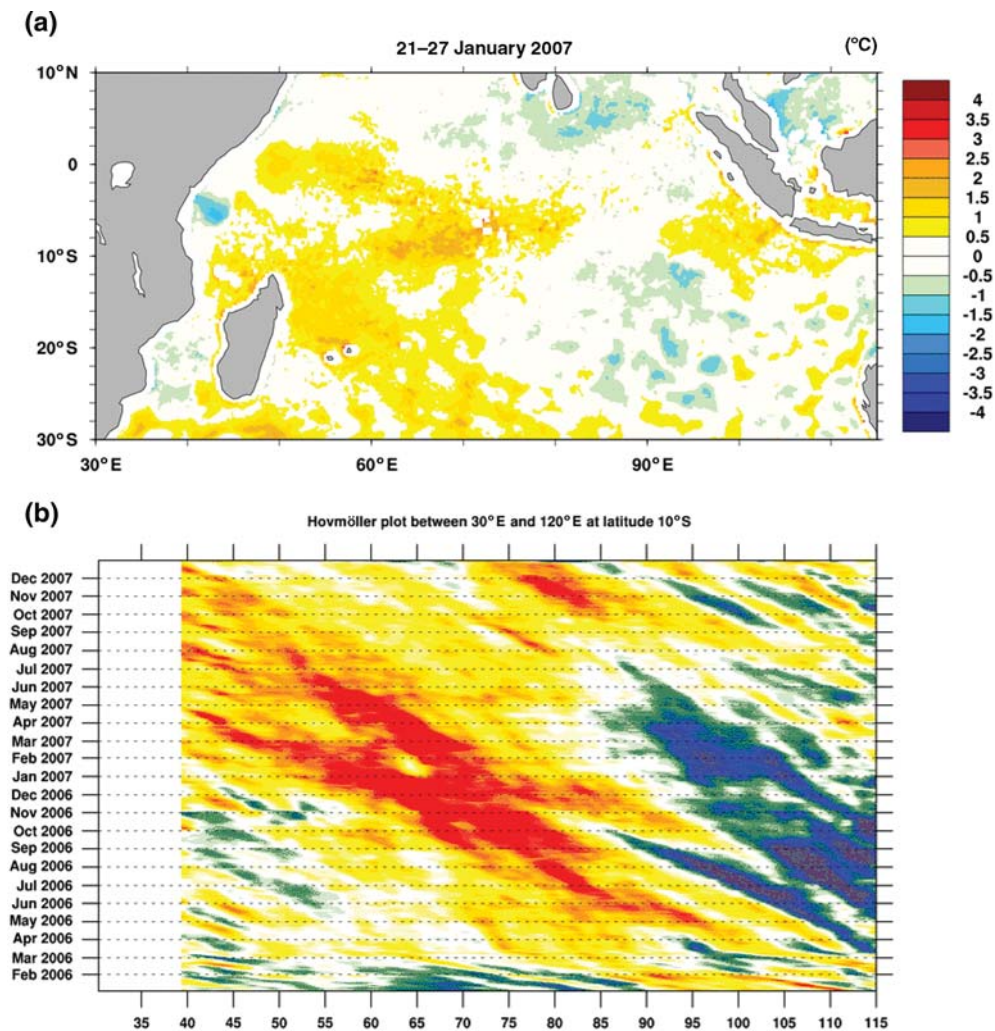


**Figure 6.** (a) Weekly (21–27 January 2007) sea surface temperature anomaly from the monthly mean over the Southwest Indian Ocean from the AVHRR data. (b) Hovmöller plot of the TOPEX/ERS2 sea surface height anomaly at 10°S from a monthly mean for 2006/2007.

austral winter 2006 to summer 2007. Sea surface height data (a proxy for upper-ocean heat content; Figure 6b), retrieved from TOPEX/ERS2 satellite observations, indicate that such a wave was generated near 90–95°E in May/June 2006 and propagated across the tropical South Indian Ocean to near 50–55°E by January/February 2007. In doing so, it deepened the thermocline, resulting in the core region of the SCTR becoming substantially deeper in the austral summer 2006/2007. The associated increase in upper-ocean heat content, and SST, was therefore very favourable for the generation and intensification of tropical storms there. Figure 6b also shows the depression in sea surface height in the EIO during the austral winter and spring of 2006, because of the strong IOD-related cooling.

Figure 6b also suggests the presence of a secondary Rossby-wave feature, generated near 90°E in November 2006, which seems to have merged with the primary feature near 70–75°E in December 2006/January 2007, before separating from it near 60–65°E in January/February 2007. This behaviour could have stemmed from the anomalous atmospheric conditions that developed over the SWIO at the time, and which affected TC Favio strongly. The latter intensified from a tropical storm to a category 3 TC when it moved southwestwards. There were ten other named storms during the austral summer 2006/2007, seven of which were TCs (six were classified as intense TCs). Although atmospheric factors are very important for storm formation, it is interesting that nine of these storms formed over or close to the core region of the SCTR, to the east of Madagascar in the SWIO (Klinman and Reason, 2008; [http://www.metoffice.gov.uk/weather/tropicalcyclone/tctracks/swi06\\_7.gif](http://www.metoffice.gov.uk/weather/tropicalcyclone/tctracks/swi06_7.gif)). In addition, the fact that six of the storms reached intense TC status indicates above-average activity, although the total number of TCs in the

SWIO in the 2006/2007 austral summer (ten) is only slightly above the average of nine.

The 2006/2007 warming was captured in detail during the Vasco-Cirene cruise and has been described in greater detail using results from the ATLAS mooring deployed then, as well as Argo floats (Vialard *et al.*, 2009). The anomalous deepening of the SCTR in the austral summer 2006/2007 has further been related to low surface chlorophyll concentrations and to a larger than normal vertical habitat for tuna, resulting in a decrease in catches (Vialard *et al.*, 2009). It has also been suggested that rainfall over the Western Ghats of India was effected on by the unusual 2007 Indian monsoon, brought about by air–sea interaction over the SCTR (Izumo *et al.*, 2008; Vialard *et al.*, 2009; Resplandy *et al.*, unpublished data).

To investigate the interannual variability of these Rossby-wave signals, ECCO (www.ecco-group.org) model temperatures at a depth of 65 m are displayed in a Hovmöller transect across the Indian Ocean to the Coral Sea at 9.5°S for the past 20 years (Figure 7). The strong 2006/2007 downwelling wave is evident at the top of the plot, as are those associated with the *El Niño* events of 1982/1983, 1993/1994, 1994/1995, 1997/1998, and 2002/2003, whereas there is less evidence of such a wave in the 1991/1992 and 1986/1987 *El Niño* events. The 2006/2007 *El Niño* event was relatively weak, but the associated downwelling Rossby wave was one of the strongest in the ECCO data, because of the positive-phase IOD event occurring simultaneously. There was another strong downwelling wave in 1997/1998, also an *El Niño* event coinciding with a positive-phase IOD event. This enhanced Rossby-wave activity, and warming in the SCTR during the austral summer 2006/2007, was very favourable for TC activity in the SWIO, as observed during that period.

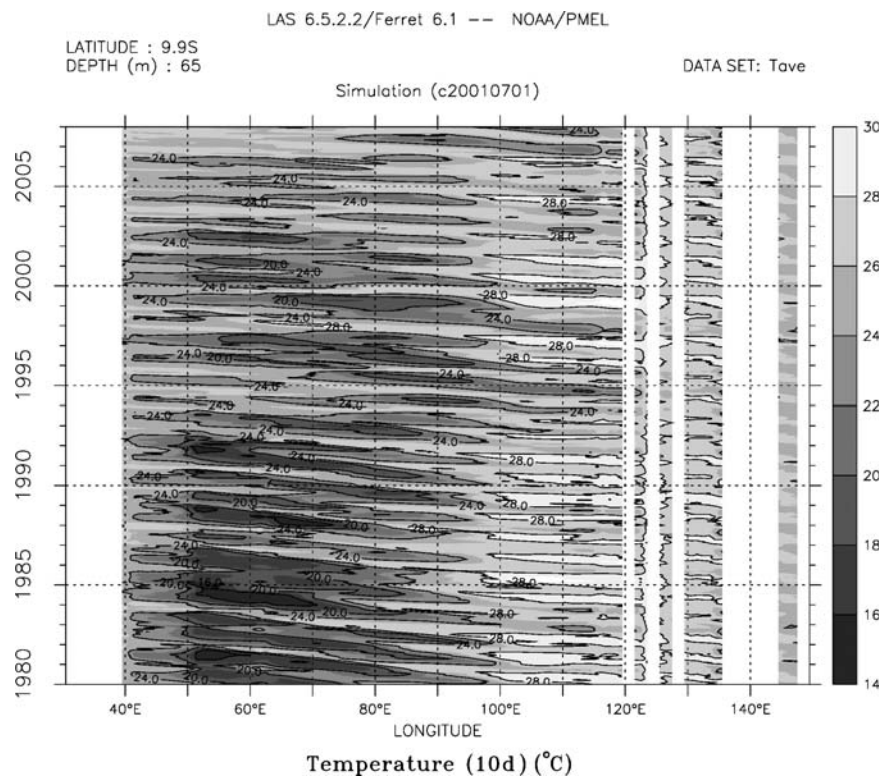


Figure 7. ECCO model subsurface (65 m) sea temperature over the Indian Ocean at 9.5°S from 1980 to 2008.

The upwelling cold Rossby waves associated with the 1988/1989, 1995/1996, and 1998/1999 *La Niña* events are evident in Figure 7. Within the entire record, 1998/1999 stands out as a strong upwelling Rossby-wave event that occurs across almost the entire transect. During the 1998/1999 cyclone season, there were only two TCs. A slight warming is evident in early summer 2000 (also a *La Niña* year), particularly in the central to eastern parts of the basin. This season was also characterized by some strong TCs, including TC Eline that was generated near 100°E and tracked more or less due west to Mozambique, because of a very strong west-steering current, and it has been one of the longest lived TCs in the basin to date (Reason and Keibel, 2004). Figure 7 suggests that the SCTR was close to, or perhaps deeper than, average during early 2000, which together with the positive SST anomalies occurring farther south of the section (Figure 7) were favourable for TC Eline.

Although beyond the scope of this study, it is also apparent from Figure 7 that the 1982–1993 period was characterized by more cool events in the central to western Indian Ocean, and upwelling Rossby waves than the last decade. NCEP windstress curl over the SCTR region (not shown) has tended to reduce in strength from 1995 to date, compared with the period 1980–1995. A reduction in the windstress curl would have resulted in a reduction in the upwelling in this region and hence the warmer temperatures seen in Figure 7 in the recent period.

## Summary and discussion

The SCTR is a prominent shoaling of the thermocline ridge in the tropical South Indian Ocean. Both the local Ekman upwelling and remote forcing (e.g. Rossby waves) contribute to its evolution. Its seasonality, which includes a prominent semi-annual cycle, has only recently been studied in depth (Hermes and Reason, 2008; Yokoi *et al.*, 2008). Variations in its depth have been linked to changes in the Indian monsoon and to TC activity, intraseasonal oscillations, and chlorophyll concentrations in the region. Therefore, a better understanding of its sensitivity in strength and location to changes in forcing is important.

This study has used a regional ocean model (ROM) to investigate the response of the SCTR to latitudinal shifts in the mean windforcing over the South Indian Ocean and to changes in the strength of these winds, as well as to explore the influence of remote forcing on the open ocean upwelling region. Using various idealized experiments, we have provided evidence of the importance of local and remote winds on the passage of Rossby waves in the Indian Ocean. A summary of the main results is presented in Table 1.

The model results suggest that a strong semi-annual cycle in the SCTR depth depends on the curl between the equatorial westerlies north of Madagascar and the subtropical easterlies, because this cycle essentially disappears when the anticyclone is shifted either north or south by 2°. The location of the SCTR appears to respond linearly to shifts in the mean basin-scale winds. A doubling in intensity of the mean winds results in a more or less proportional increase in the amplitude of its annual cycle during the first half of the year, but not during the late austral winter and spring, when more rapid changes in thermocline depth occur than in the CON.

There is little effect on the propagation of Rossby waves if the major topographic features in the STIO are removed. If coarser resolution NCEP winds are used, the thermocline becomes deeper in the austral winter and does not extend as far to the

east, although there is little difference in summer. An increase in the depth of the average thermocline occurs if the winds are strengthened over the ridge; however, the breakdown in the Rossby waves at 65–70°E is enhanced. Doubling the remote winds in the EIO has a strong effect on the depth of the thermocline ridge in the SCTR region, deepening the thermocline here and slowing down the west-propagating, upwelling Rossby waves. This result highlights the significance of remote forcing for the SCTR. To better understand the sensitivity of these Rossby waves to global climate signals and the possible effect on the SCTR, it would be useful to extend this study using a high-resolution global model.

Further exploration of the effect of Rossby waves on the SCTR was done using the 2006/2007 austral summer as a case study. As expected (from work by Xie *et al.*, 2002), the thermocline was deeper in early summer 2006/2007, before the cyclones, resulting in a higher SST over the region. This deepening occurred after the arrival of a strong downwelling wave and a reduction in the windstress curl over the SCTR. Xie *et al.* (2002) suggested that the SST variability in the western tropical South Indian Ocean (up to 50% of the total variance in certain seasons) is not locally forced, but is instead a result of these oceanic subsurface waves.

This study has highlighted the interannual variability of the SCTR and the potential contribution of Rossby waves in influencing this variability. Given the significance of the SCTR, it must be emphasized that the remaining gaps in the Indian Ocean Observing System should be filled as soon as possible. Better monitoring of both the basin-scale winds and subsurface ocean conditions is needed to improve our understanding of the SCTR and its effects on regional climate and marine biodiversity. The developing Indian Ocean Observing System ([www.clivar.org/organization/indian.php](http://www.clivar.org/organization/indian.php)) will greatly assist with this task if gaps in the moored array (RAMA) in the western Indian Ocean are filled. These gaps are mainly in the western part of the Indian Ocean and, while they exist, they hamper better understanding of the SCTR region.

## Acknowledgements

Funding received from the South African National Research Foundation helped support this study and the attendance of the lead author to the 2008 PICES/ICES conference on the effects of climate change on the world's oceans. Partial funding for attendance was also gratefully received from the World Climate Research Programme. Figure 6 was plotted on <http://realtime.sea.uct.ac.za/realtime/regions/indianOcean> and Figure 7 on the ECCO website (<http://www.ecco-group.org/>). Comments from two anonymous reviewers are gratefully acknowledged.

## References

- Allan, R. J., Lindesay, J. A., and Reason, C. J. C. 1995. Multi-decadal variability in the climate system over the Indian Ocean region during the austral summer. *Journal of Climate*, 8: 1853–1873.
- Annamalai, H., Liu, P., and Xie, P. 2005. Southwest Indian Ocean SST variability: its local effect and remote influence on Asian monsoons. *Journal of Climate*, 18: 4150–4167.
- Annamalai, H., Murtugudde, R., Potemra, J., Xie, S-P., Liu, P., and Wang, B. 2003. Coupled dynamics over the Indian Ocean: spring initiation of the zonal mode. *Deep Sea Research*, 50: 2305–2330.
- Behera, S. K., Salvekar, P. S., and Yamagata, T. 2000. Simulation of interannual SST variability in the tropical Indian Ocean. *Journal of Climate*, 13: 3487–3499.

- Behera, S. K., and Yamagata, T. 2001. Subtropical SST dipole events in the southern Indian Ocean. *Geophysical Research Letters*, 28: 327–330.
- Birol, F., and Morrow, R. 2001. Source of the baroclinic waves in the Southeast Indian Ocean. *Journal of Geophysical Research*, 106: 9145–9160.
- Conkright, M. E., Locarnini, R. A., Garcia, H. E., O'Brien, T. D., Boyer, T. P., Stephens, C., and Antonov, J. I. 2002. World Ocean Atlas 2001: objective analyses, data statistics and figures, CD-ROM documentation. National Oceanographic Data Centre, Silver Spring, MD. 17 pp.
- Duvel, J. P., Roca, R., and Vialard, J. 2004. Ocean mixed layer temperature variations induced by intraseasonal convective perturbations over the Indian Ocean. *Journal of Atmospheric Sciences*, 61: 1004–1023.
- Duvel, J.-P., and Vialard, J. 2007. Indo-Pacific sea surface temperature perturbations associated with intraseasonal oscillations of the tropical convection. *Journal of Climate*, 20: 3056–3082.
- Gallienne, C. P., and Smythe-Wright, D. 2005. Epipelagic mesozooplankton dynamics around the Mascarene Plateau and Basin, south-western Indian Ocean. *Philosophical Transactions of the Royal Society A*, 363: 191–202. doi:10.1098/rsta.2004.1487.
- Hermes, J. C., and Reason, C. J. C. 2005. Ocean model diagnosis of interannual coevolving SST variability in the South Indian and South Atlantic Oceans. *Journal of Climate*, 18: 2864–2882.
- Hermes, J. C., and Reason, C. J. C. 2008. Annual cycle of the South Indian Ocean (Seychelles–Chagos) thermocline ridge in a regional ocean model. *Journal of Geophysical Research*, 113: C04035. doi:10.1029/2007JC004363.
- Izumo, T., de Boyer Montegut, C., Luo, J.-J., Behera, S. K., Masson, S., and Yamagata, T. 2008. The role of the western Arabian Sea upwelling in Indian monsoon rainfall variability. *Journal of Climate*, 21: 5603–5623.
- Jury, M. R., Pathack, B., and Parker, B. 1999. Climatic determinants and statistical prediction of tropical cyclone days in the Southwest Indian Ocean. *Journal of Climate*, 12: 1738–1746.
- Kalnay, E., Kanamitsu, M., Kistler, R., Collins, W., Deaven, D., Gandin, L., Iredell, M., *et al.* 1996. The NCEP/NCAR 40-year reanalysis project. *Bulletin of the American Meteorological Society*, 77: 437–495.
- Klinman, M., and Reason, C. J. C. 2008. On the peculiar storm track of TC Favio during the 2006–2007 Southwest Indian Ocean tropical cyclone season and relationships to ENSO. *Meteorology and Atmospheric Physics*, 100: 233–242.
- Liu, W. T., Tang, W., and Polito, P. S. 1998. NASA scatterometer global ocean-surface wind fields with more structures than numerical weather prediction. *Geophysical Research Letters*, 25: 761–764.
- Masumoto, Y., and Meyers, G. 1998. Forced Rossby waves in the southern tropical Indian Ocean. *Journal of Geophysical Research*, 103: 27589–27602.
- Matano, R. P., Beier, E. J., Strub, P. T., and Tokmakian, R. 2002. Large-scale forcing of the Agulhas variability: the seasonal cycle. *Journal of Physical Oceanography*, 32: 1228–1241.
- McCreary, J. P., Kundu, P. K., and Molinari, R. L. 1993. A numerical investigation of dynamics, thermodynamics and mixed-layer processes in the Indian Ocean. *Progress in Oceanography*, 31: 181–244.
- New, A. L., Stansfield, K., Smythe-Wright, D., Smeed, D. A., Evans, A. J., and Alderson, S. G. 2005. Physical and biochemical aspects of the flow across the Mascarene Plateau in the Indian Ocean. *Philosophical Transactions of the Royal Society A*, 363: 151–168. doi:10.1098/rsta.2004.1484.
- Penven, P., Marchesiello, P., Debret, L., and Lefèvre, J. 2008. Software tools for pre- and post-processing of oceanic regional simulations. *Environmental Modelling and Software*, 23: 660–662.
- Rao, R. R., and Sivakumar, R. 1998. Observed seasonal variability of heat content in the upper layers of the tropical Indian Ocean from a new global ocean temperature climatology. *Deep Sea Research*, 45: 67–89.
- Rao, R. R., and Sivakumar, R. 2000. Seasonal variability of near-surface thermal structure and heat budget of the mixed layer of the tropical Indian Ocean from a new global ocean temperature climatology. *Journal of Geophysical Research*, 105: 995–1015.
- Rao, S. A., and Behera, S. K. 2005. Subsurface influence on SST in the tropical Indian Ocean: structure and interannual variability. *Dynamics of Atmospheres and Oceans*, 39: 103–135.
- Rao, S. A., Behera, S. K., Masumoto, Y., and Yamagata, T. 2002. Interannual subsurface variability in the tropical Indian Ocean with a special emphasis on the Indian Ocean dipole. *Deep Sea Research*, 49: 1549–1572.
- Reason, C. J. C. 2001. Subtropical Indian Ocean SST dipole events and southern African rainfall. *Geophysical Research Letters*, 28: 2225–2227.
- Reason, C. J. C., Allan, R. J., Lindesay, J. A., and Ansell, T. J. 2000. ENSO and climatic signals across the Indian Ocean Basin in the global context: part I, interannual composite patterns. *International Journal of Climatology*, 20: 1285–1327.
- Reason, C. J. C., and Keibel, A. 2004. Tropical cyclone Eline and its unusual penetration and impacts over the southern African mainland. *Weather and Forecasting*, 19: 789–805.
- Saji, N. H., Goswami, B. N., Vinayachandran, P. N., and Yamagata, T. 1999. A dipole mode in the tropical Indian Ocean. *Nature*, 401: 360–363.
- Sakova, I., Meyers, G., and Coleman, R. 2006. Interannual variability in the Indian Ocean using altimeter and IX1-expendable bathy-thermograph (XBT) data: does the 18-month signal exist? *Geophysical Research Letters*, 33: L20603. doi:10.1029/2066GL027117.
- Schott, F. A., and McCreary, J. P. 2001. The monsoon circulation of the Indian Ocean. *Progress in Oceanography*, 51: 1–123.
- Shchepetkin, A. F., and McWilliams, J. C. 2005. The regional oceanic modeling system (ROMS): a split-explicit, free-surface, topography-following-coordinate oceanic model. *Ocean Modeling*, 9: 347–404.
- Vialard, J., Duvel, J. P., McPhaden, M. J., Bouruet-Aubertot, P., Ward, B., Key, E., Bourras, D., *et al.* 2009. Air–sea interactions in the Seychelles–Chagos thermocline ridge region. *Bulletin of the American Meteorological Society*, 90: 45–61.
- Vinayachandran, P. N., Iizuka, S., and Yamagata, T. 2002. Indian Ocean dipole mode events in an ocean general circulation model. *Deep Sea Research II*, 49: 1573–1596.
- Vitart, F., Anderson, D., and Stockdale, T. 2003. Seasonal forecasting of tropical cyclone landfall over Mozambique. *Journal of Climate*, 16: 3932–3945.
- Wang, L., Koblinsky, C. J., and Howden, S. 2001. Annual Rossby wave in the southern Indian Ocean: why does it “appear” to break down in the middle ocean? *Journal of Physical Oceanography*, 31: 54–74.
- Washington, R., and Preston, A. 2006. Extreme wet years over southern Africa: role of Indian Ocean sea surface temperatures. *Journal of Geophysical Research*, 111: D15104. doi:10.1029/2005JD006724.
- Webster, P. J., Moore, A. M., Loschnigg, J. P., and Leben, R. R. 1999. Coupled ocean–atmosphere dynamics in the Indian Ocean during 1997–98. *Nature*, 401: 356–360.
- Xie, S.-P., Annamalai, H., Schott, F. A., and McCreary, J. P. 2002. Structure and mechanism of South Indian Ocean climate variability. *Journal of Climate*, 15: 864–878.
- Yokoi, T., Tozuka, T., and Yamagata, T. 2008. Seasonal variation of the Seychelles Dome. *Journal of Climate*, 21: 3740–3754. doi:10.1093/icesjms/fsp074